Dalton Transactions

Accepted Manuscript

This article can be cited before page numbers have been issued, to do this please use: M. Irfanullah, A. Chowdhury and N. Bhardwaj, *Dalton Trans.*, 2016, DOI: 10.1039/C6DT01917J.

ROYAL SOCIETY OF CHEMISTRY

www.rsc.org/dalton

ROYAL SOCIETY OF CHEMISTRY
View Article Online
DOI: 10.1039/C6DT01917J

Journal Name

ARTICLE

Sensitized luminescence from water-soluble LaF_3:Eu nanocrystals via partially-caped 1,10-phenanthroline: time-gated emission and multiple lifetimes†

Received 00th January 20xx,
Accepted 00th January 20xx

DOI: 10.1039/x0xx00000x

www.rsc.org/

Mir Irfanullah, Navneet Bhardwaj, Arindam Chowdhury*

Water dispersible citrate-capped LaF_3:Eu(5%) nanocrystals (NCs) have been partially surface-functionalized by 1,10-phenanthroline (phen) via ligand exchange method to produce novel water dispersed citrate/phen-capped LaF_3:Eu(5%) NCs in which citrate ligands preserve the water dispersibility of the NCs and phen ligands act as sensitizers of surface Eu^{3+}-dopant sites. The partial ligand exchange and the formation of water dispersed NCs has been monitored by ^1H NMR spectroscopy, as well as luminescence measurements at different time intervals during the reaction. These NCs display a distinct phen-sensitized Eu^{3+}-emission profile with enhanced intensity in water as compared to the emission profile and intensity obtained upon direct excitation. Time-gated emission spectroscopy (TRES) has been used to probe PL dynamics of Eu^{3+}-sites of LaF_3:Eu(5%) NCs by taking advantage of selectively sensitizing surface Eu^{3+}-dopant sites by phen ligands as well as by exciting all the Eu^{3+}-sites in the NCs upon direct excitation. TRES upon direct excitation of the citrate-capped LaF_3:Eu(5%) NCs reveals that Eu^{3+}-dopants occupy at least three different sites, each with a different emission profile and lifetime, and emission from purely interior Eu^{3+}-sites has been resolved due to their long lifetime as compaed to the lifetime of purely surface and near surface Eu^{3+}-sites. On the contrary, the phen-sensitized emission from citrate/phen-capped LaF_3:Eu(5%) NCs display similar emision profiles and lifetimes in TRES measurements, which reveals that phen truly sensitizes purely surface dopant sites of the NCs in water, all of which have nearly same local environment. The phen–sensitized Eu^{3+}-emission of the NCs in water remains stable even upon addition of various buffer solutions at physiological pH, as well as upon addition of water-miscible organic solvents. Further, the two-photon excitation ($\lambda_{ex.}$ = 720 nm) of these water-soluble phen-capped NCs produces bright red Eu^{3+} emission, which reveals that these NCs are promising for potential applications in biological imaging.

Introduction

Lanthanide (Ln)-doped nanoparticles show unique photoluminescence (PL) properties, such as bright emission with narrow full width at half maxima (FWHM), multicolour/tunable emission, photostability/non-blinking behavior at single-particle levels, and long-lived PL lifetimes.[1] Because of these properties, they find a wide range of applications such as luminescent probes in biological imaging, sensors, display devices and spectral converters for enhancing solar cell efficiency.[2] The long PL lifetimes (micro- to milliseconds) of Ln-doped nanoparticles are especially more valuable for applications such as in time-resolved PL imaging of biological samples, where exceptionally high contrast is achieved due to suppression of the autofluorescence (lifetime < 10 ns) from the background/sample.[3] Radovanovic and co-workers have recently demonstrated that the millisecond lifetimes of the dual emissions arising from Ln^{3+} dopants and their host in colloidal Ln-doped Ga_2O_3 nanocrystals (NCs) can be temporally modulated to achieve PL chromacity tuning on the millisecond timescale.[4] Moreover, it was also recently shown that the microsecond lifetimes of the $NaYF_4$:Yb,Er and $NaYF_4$:Yb,Tm upconversion nanoparticles (or τ-dots) could be tuned by varying the size of the particles, or by varying the thulium (dopant) concentration, respectively,[5] and their tunable lifetimes have been coded for optical multiplexing which offers a new temporal dimension of optical codes for data storage, document security and multiplexing assays.[5a]

The synthesis of Ln-doped nanoparticles is achieved by various methods, many of which allow accurate control of the morphology, composition, crystal phase, as well as the emission colors of the particles.[6] A variety of organic ligands are attached to the surface of these nanoparticles to make them easily dispersible in both aqueous as well as non-aqueous media. The dissolution of luminescent nanomaterials in aqueous media is essential for their applications in biological imaging.[2a] Recent synthetic efforts have also produced many

Department of Chemistry, Indian Institute of Technology Bombay, Powai, Mumbai, 400076, India. E-mail: arindam@chem.iitb.ac.in; Fax: +91-2225767152; Tel: +91-2225767154

†Electronic Supplementary Information (ESI†) available: Additional TEM images and ^1H NMR spectra, TGA plot and luminescence measurements at different time intervals during the formation of citrate/phen-capped LaF_3:Eu NCs in water. See DOI: 10.1039/x0xx00000x

Ln-doped nanoparticles in which organic surface capping ligands have been employed as sensitizers of the dopant sites, which has enabled more efficient luminescence from these nanomaterials.[7,8]

However, there are very few reports available in the existing literature on water-dispersible Ln-doped nanoparticles demonstrating the strategy of surface-capped organic-ligand sensitized luminescence from dopants.[7c,d,8c] The development of efficiently luminescent water-dispersible nanoparticles is a hot topic of the biomedical research,[9] and considering the increasing popularity of Ln-doped nanoparticles and their potential applications, it is important to extend this strategy of surface sensitization to develop water dispersible nanoparticles, which could be useful for biological imaging.[3,8c]

Further, surface sensitized Ln-doped nanoparticles reported in the literature so far are limited to oxygen(O)-donor ligands (such as β-diketonates),[7,8] and to the best of our knowledge Ln-doped nanoparticles surface capped with nitrogen(N)-donor organic ligand sensitizers for Ln^{3+} dopant sites are yet to be reported. Lanthanides being hard acids are traditionally known to prefer O-donor ligands as compared to N-donor ligands for coordination. However, many novel lanthanide complexes with N-donor ligands, especially with a chelating site have been reported in the literature, which are much efficient sensitizers of lanthanide luminescence as compared to many O-donor ligands.[10] There are various N-donor ligands which can be employed as surface capping ligands and potential sensitizers of dopant sites in Ln-doped nanoparticles. Among them, 1,10-phenanthroline (phen) is one of the N-donor ligands which can be explored as surface capped sensitizer in Ln-doped nanoparticles because of its following merits, i) it is versatile NN donor ligand and has been extensively used for making luminescent materials with a range of metal ions including lanthanides,[11] ii) it has a rigidly planar structure and entropically favourable chelating capability, and its coordination complexes with trivalent lanthanides can be isolated even in aqueous medium,[12] iii) phen is a weak fluorescent molecule itself, but it has been proved to be an excellent sensitizer of the europium emission with its coordination complexes and hybrid materials,[13] iv) phen is moderately soluble in water, but its solubility in aqueous medium increases significantly with increase in temperature,[14] which can be exploited to perform reactions of phen with metal ions and nanoparticles surfaces in water at moderately higher temperatures, and v) phen is cheaply available commercially and does not need to be synthesized which saves time and energy while investigating its luminescent materials with metal ions and nanoparticles. Recently, electrochemically deposited Eu^{3+}-embedded ZnO nanowall structures deposited on ITO-glass and further coated with phen have been reported by Leung and co-workers, in which a unique cascade energy transfer model involving ZnO, phen and Eu^{3+} ions has been proposed.[15]

Time-resolved (or time-gated) emission spectroscopy (TRES) in an important technique by which a detailed understanding of the PL dynamics of Ln^{3+} dopants in different coordinating sites (surface-bound vs. internally incorporated sites) of the NCs can be obtained.[4] Two or more environmentally different Ln^{3+} dopant emitters in a NC matrix can be distinguished through TRES by taking advantage of their long luminescence lifetimes (μs to ms range), and by exploiting the possible variations in the lifetimes of these different dopant emitters. Significant differences in the lifetimes of different dopant emitters can be helpful in resolving their pure emission spectra, while very close lifetimes will lead to overlapping spectra from different dopant sites. However, if some of the dopant sites such as surface Ln^{3+} sites can be selectively excited using surface capping organic ligands, TRES can be extremely useful in understanding the PL dynamics of the Ln^{3+} sites in Ln-doped NCs.

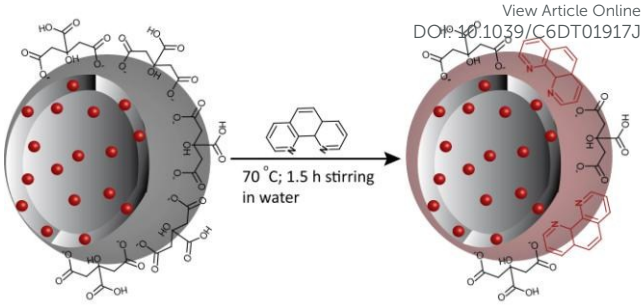

Figure 1. A schematic representation of a partial exchange of citrate capping ligands of LaF_3:Eu(5%) nanocrystals by 1,10-phenanthroline in water, at 70 °C. The red dots represent Eu^{3+} dopant sites in LaF_3 NC matrix.

In this work, we report the interaction of water dispersed citrate-capped LaF_3:Eu(5%) NCs with a saturated aqueous solution of phen at 70 °C, which strikingly results in partial replacement of O-donor citrate capping ligands of the NCs by neutral NN-donor phen ligands as shown in Figure 1. The resulting citrate/phen-capped LaF_3:Eu(5%) NCs despite containing phen capping ligands are dispersed in water and show distinct emission profiles and lifetimes of Eu^{3+}-dopant sites upon direct-excitation, and sensitization by partially surface-capped phen ligands. The luminescence from citrate/phen-capped LaF_3:Eu(5%) NCs has been compared with $[Eu(phen)_2(NO_3)_3]$ complex, and in both the materials phen sensitization gives is more intense emission as compared to direct excitation. Further, taking advantage of the long luminescence lifetimes of Eu^{3+} dopant sites and selective sensitization of surface dopant sites by phen, we have investigated PL dynamics of different Eu^{3+}-dopant sites of the NCs by using TRES. Our motivation is to investigate the luminescence properties of purely surface and interior Eu^{3+}-dopant sites of the LaF_3:Eu(5%) NCs, and our results clearly show that the luminescence profiles and lifetimes of purely surface and interior dopants are distinctively different. The stability of phen-sensitized Eu^{3+}-emission, and preliminary two-photon excited PL imaging of citrate/phen-capped LaF_3:Eu(5%) NC aggregates is presented.

Experimental section

Materials. All the chemicals and solvents used in this study were used as received, unless otherwise specified.

$La(NO_3)_3{\cdot}6H_2O$ (≥99.0%), $Eu(NO_3)_3{\cdot}5H_2O$ (99.9%), NaF (99.9%), citric acid (≥99.5%), ammonia (≥ 25% in H_2O) were purchased from Sigma Aldrich. 1,10-Phenanthroline was purchased from Merck, India. The solvents used in the synthesis, and in spectroscopy measurements of were either synthetic grade or spectroscopy grade, and were purchased either from Sigma-Aldrich or Spectrochem India. The $[Eu(phen)_2(NO_3)_3]$ complex was synthesized according to a slightly modified procedure reported in the literature,[13c] (ESI†).

Citrate-capped LaF_3:Eu(5%) NCs. These NCs were synthesized according to a slightly modified procedure reported in literature.[7d] An aqueous solution of 2.00 g (10.4 mmol) of citric acid was dissolved in 40 mL of millipure water and partially neutralized with dropwise addition of ammonia (25% solution in H_2O) until the pH reached 5.7. The solution was heated to 95 °C on a water bath while stirring with magnetic stirrer. A solution of 0.55 g (1.3 mmol) of $La(NO_3)_3{\cdot}6H_2O$ and 0.027 g (0.061 mmol) of $Eu(NO_3)_3{\cdot}5H_2O$ in 6 mL of methanol was added dropwise to the above citrate solution under stirring, followed by the dropwsie addition of a solution of 0.18 g (4.3 mmol) of NaF in 6 mL of millipure H_2O. The reaction mixture was stirred continuously for 2 h at 95 °C and then allowed to cool to room temperature. The addition of 50 mL of absolute ethanol to the above reaction mixture resulted in the precipitation of the NCs in water/ethanol mixture, which were immediately separated by centrifugation. The resulting white precipitates of NCs were further washed thoroughly with absolute ethanol and dried under vacuum overnight. These NCs are easily redispersible in water due to surface capping citric acid.

Citrate/phen-capped LaF_3:Eu(5%) NCs. The citrate-capped LaF_3:Eu(5%) NCs (100 mg) were dispersed in 20 mL of water and heated to 70 °C. To this dispersion of NCs in water was added a saturated solution of phen in water (250 mg of phen in 10 mL H_2O) at 70 °C. The mixture was continuously stirred for 2 hours at 70 °C. After 15 minutes, the mixture of NCs and phen in water changes from colorless to light reddish-orange in color, and the color brightens as the reaction proceeds up to 1.5 h. After 2 h stirring at 70 °C, the aqueous mixture was cooled to room temperature, which results in the precipitation of excess phen ligand. These white precipitates of phen were separated through centrifugation and the resulting clear reddish-orange dispersion of the NCs was kept in the refrigerator for 6 hours at 10 °C, which resulted in the precipitation of remaining minute amounts of unreacted phen dissolved in water. These phen precipitates were again removed through centrifugation and the resulting clear dispersion of the surface modified NCs in water was found to be stable for few days, and was used as such for PL measurements. The reaction was repeated several times to ensure reproducibility of the results. A similar reaction was done in D_2O, but with lower amounts of citrate-capped LaF_3:Eu(5%) NCs (20 mg in 4 mL D_2O) and phen (50 mg in 2 mL D_2O), for NMR measurements.

Sample characterization

Powder X-ray diffraction (XRD) pattern of the NCs was recorded on a Philips powder diffractometer PW3040/60 with Cu Kα (0.15406 nm) radiation. Transmission electron microscopy (TEM) images and energy dispersive X-ray (EDX) spectroscopy of the NCs were performed with a PHILIPS CM200 microscope with operating voltages 20-200 kV and resolution of 2.4 Å. The sample was prepared by drop-casting the NCs dispersed in water on a carbon-coated copper grid. The solvent was allowed to evaporate for 2 hours and finally grid was dried by heating with IR lamp. Thermogravimetric analysis (TGA) was carried out on a Perkin-Elmer Pyris thermal analysis system under a nitrogen atmosphere at a heating rate of 10 °C/min. The ^{1}H NMR spectra were recorded by 500 MHz Bruker Avance III spectrometer. Chemical shift data are quoted as δ in ppm, and the singlet, doublet, triplet and broad resonances are denoted as *s*, *d*, *t* and *b*, respectively. The UV-vis absorption spectra were recorded at room temperature on a JASCO V 530 spectrophotometer, using standard quartz cuvettes of 1 cm pathlength. The steady-state emission and excitation spectra were recorded at room temperature on Varian Cary Eclipse spectrofluorimeter, using standard quartz fluorescence cuvettes of 1 × 1 cm pathlength. The time-gated emission spectra of the NCs were recorded on Varian Cary Eclipse spectrofluorimeter by using various time delays varying between 0.1 to 25 ms range and a fixed gate time. The decay curves were obtained by monitoring delay times *vs*. integrared intensity of the $^5D_0 \rightarrow {}^7F_1$ emission (592 nm) as well as $^5D_0 \rightarrow {}^7F_2$ emission (616 nm), respectively. The decays were either single exponential or tri-exponential and were analyzed with OriginPro 8 software. The average lifetime ($\tau_{avg.}$) of the tri-exponential decay curves was obtained by using the formula: $\tau_{avg.} = (\tau_1 \times A_1 + \tau_2 \times A_2 + \tau_3 \times A_3)/(A_1+A_2+A_3)$. The two-photon excited images were collected on a Carl Zeiss LSM-780 confocal microscope equipped with a two-photon coherent chameleon pulsed Ti:sapphire laser. The emission was collected using 594-668 nm filter.

Results and discussion

Synthesis and characterization

Water dispersible LaF_3:Eu(5%) NCs were synthesized according to a slightly modified procedure reported in the literature,[7d] in which La^{3+}, Eu^{3+} and F^- precursors were added in quick succession to the neutralized citrate ion solution in water, and constantly stirred for 2 hours around 90-95 °C (~25 °C higher than the published procedure). The isolated NCs are easily redispersible in water due to surface-capped citrate ligands. The phase structure of as-synthesized NCs was studied by powder X-ray diffraction as shown in Figure 2, along with International Centre for Powder Diffraction Data (ICCD) file for LaF_3 (01-082-0690). From the observed diffraction pattern, the phase structure of these NCs can be easily indexed to the pure tysonite structure of the LaF_3 with $P\overline{3}c1$ space group. Further, the broadening of diffraction peaks reveals the crystalline nature of the sample with a very small size. A similar broad diffraction pattern can be observed in ultra-small Eu^{3+}-doped LaF_3 NCs reported in the literature.[7d,e,16]

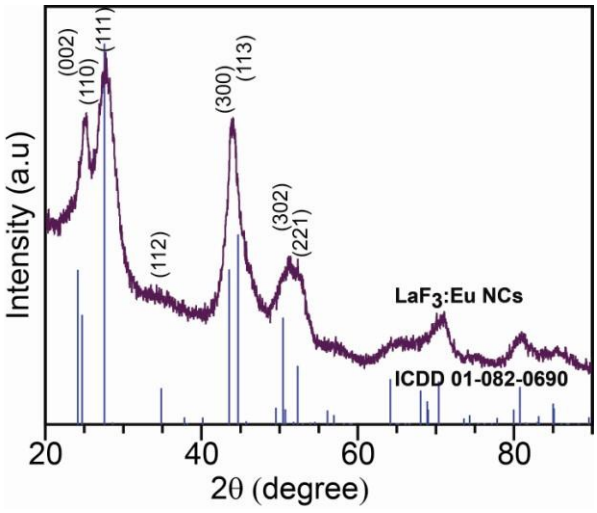

Figure 2. Powder X-ray diffraction of citrate-capped LaF_3:Eu(5%) NCs along with crystallographic pattern of pure LaF_3 tysonite (ICCD: 01-80-0690).

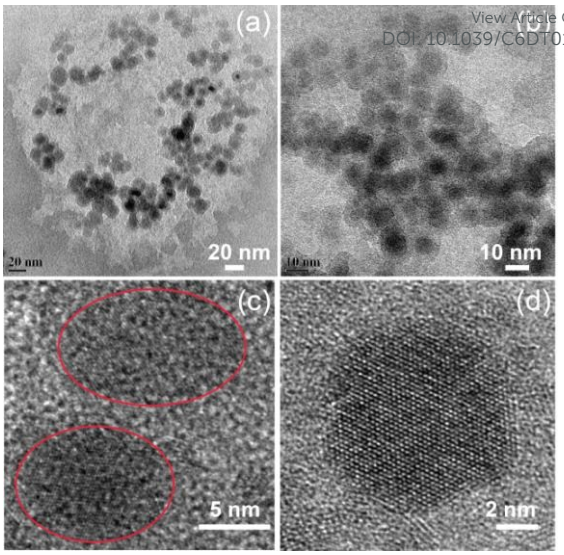

Figure 3. TEM images of citrate-capped LaF_3:Eu(5%) NCs (a, b and c). The higher resolution TEM image of a representative NC (d) shows very clear and well grown lattice fringes.

The transmission electron microscopy (TEM) measurements of the NCs were carried out to study their size and morphology, as well as confirm their crystalline nature which is revealed by powder X-ray diffraction. Figure 3 shows the representative TEM images of the NCs which have been obtained by drop-casting the sample on a carbon-coated copper grid from a dilute water-dispersion. The TEM images show that the individual particles are quasi-spherical in shape and are observed in agglomerated form (Figure S1, ESI†). Such agglomeration is often encountered in lanthanide-doped LaF_3 NCs in aqueous and some non-aqueous solvents.[16,17,18] The agglomeration of LaF_3 nanoparticles in aqueous medium is believed to occur during the evaporation process of solvent on a carbon-coated copper grid,[17a,18] because water takes longer time to evaporate unlike organic solvents which evaporate quickly. Further, there is a diffuse cloud around the primary particles, as well as different contrast between the them, which is possibly due to high concentration of the NCs on the grid because of which two or more layers of the NCs are stacked over each other. Diffuse clouding around the NCs in the literature is also attributed to the large amounts of strongly capping ligands around the primary particles.[19] Nonetheless, high-resolution (HR)-TEM images of the individual NCs (Figure 3d; and Figure S2, ESI†) show very clear and well grown lattice fringes which is in agreement with the powder X-ray diffraction pattern and confirms their highly crystalline in nature. TEM size analysis carried out on 174 individual NCs (Figure S3, ESI†) from different TEM images of a same sample preparation at different locations show that these NCs have diameters in the range of 4-16 nm, with average diameter of 9 nm.

TGA was performed on a solid (dried) citrate-capped LaF_3:Eu(5%) NCs in order to estimate the weight percentage of citrate ligands that accounts for the total weight of NCs (Figure S4, ESI†).[20] The TGA curve of the NCs can be divided mainly into two weight loss stages in the temperature range of 30 °C to 700 °C. The first weight loss in the temperature range of 30 to ~190 °C is attributed to loss of moisture by nitrogen flow as well as loss of adsorbed water by heating, which accounts to ~7 % weight of the NCs. The second weight loss in the temperature range of ~190 °C to ~700 °C is attributed to the decomposition and loss of organic citrate ligands attached to the surface of the NCs, and which accounts for ~17 % of total weight of the NCs. Therefore, based on the TGA, we estimate that citrate ligands constitute 17-18% weight of the citrate-capped LaF_3:Eu(5%) NCs.

Ligand exchange is one of the choicest methods currently available to modify the surface-functionalization of the nanoparticles by completely or partially replacing the original capping ligands.[2a] As already mentioned in the text, phen is a strong chelating ligand and capable of coordinating with the lanthanide ions in aqueous media,[12,13c] and it has moderate solubility in water at room temperature which can be increased considerably at moderately higher temperatures.[14] Further, phen is a well known sensitizer of the europium emission in both aqueous as well as non aqueous media.[13] Therefore, as synthesized citrate-capped LaF_3:Eu^{3+}(5%) NCs which are highly dispersible in water due to citrate ligands were further treated with a saturated solution of phen ligand dissolved in water at 70 °C for 2 hours. This strikingly led to partial ligand exchange and formation of water dispersed citrate/phen-capped LaF_3:Eu(5%) NCs. The colloidal dispersions of these NCs are as clear as nanopure water (Figure S5, ESI†). The partial binding of phen ligands to the surface of NCs was monitored by ^{1}H NMR spectroscopy. Figure 4 shows the ^{1}H NMR spectrum of citrate/phen-capped LaF_3:Eu(5%) NCs dispersed in D_2O, which clearly displays the proton resonances of both phen as well as citrate ligands bound to the surface of the NCs. The surface capped phen proton resonances (observed between 7–9 ppm region) are significantly broadened as compared to the sharp proton resonances observed for free phen in D_2O (Figure S6, ESI†), while proton resonances due to surface capping citrate ligands observed between 2.4–2.7 ppm in these NCs are similar to the proton

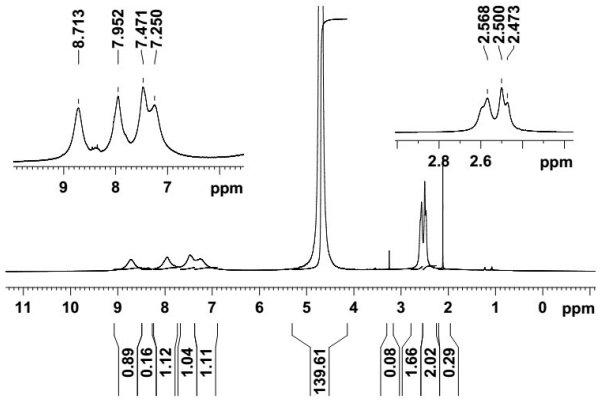

Figure 4: The ^{1}H NMR spectrum of citrate/phen-capped LaF_3:Eu(5%) NCs dispersed in D_2O. The spectrum displays proton resonances of both citrate (2.4-2.7 ppm) as well as phen capping ligands (7.0-9.0 ppm).

resonances of surface capping citrate ligands observed in citrate-only capped LaF_3:Eu(5%) NCs dispersed in D_2O (Figure S7, ESI†). The broadening of the surface bound phen proton resonances is attributed to decrease in the rotational freedom of the ligand, and inhomogeneous distribution of magnetic environment around the NCs.[21] Further, the binding of phen and ligand exchange between phen and citrate ligands on the surface of LaF_3:Eu(5%) NCs in water at different time intervals during ligand exchange reaction was also monitored by luminescence spectroscopy (Figure S8-S10, and detailed explanation of Figure S10, ESI†), which reveals that the number of phen ligands replacing citrate ligands steadily increases with time (up to 1.5 h) at constant temperature, and no further ligand exchange occurs after 1.5 hours. The attachment of neutral phen ligands (neutral NN donors) on the surface of these NCs in aqueous environment is remarkable, because these ligands have to compete with water molecules as well as already bound citrate ligands for coordination with NCs surface, which consists of hard acids (La^{3+} and Eu^{3+}) and are known to prefer hard bases such as oxygen donor ligand over nitrogen donor ligands.

It is important to note that the ratio of integrated area of phen proton resonances to the integrated area of citrate proton resonances in the ^{1}H NMR spectrum of citrate/phen-capped LaF_3:Eu(5%) NCs is 1.13:1 (Figure 4), which indicates that phen and citrate ligands are capped to the surface of NCs dispersed in water in approximately 53% and 47% proportion, respectively (in terms of number% of ligands). Further, considering that citrate ligands constitute ~18 weight% of the total weight of citrate-capped LaF_3:Eu(5%) NCs, it has been inferred that phen and citrate ligands, each constitute approximately 9% by weight of the total weight of citrate/phen-capped LaF_3:Eu(5%) NCs. It is important to mention here that due to attachment of phen ligands, water dispersed citrate/phen-capped LaF_3:Eu(5%) NCs are no longer precipitated by the addition of ethanol or many other organic solvents, unlike citrate-only capped LaF_3:Eu(5%) NCs which are easily precipitated by addition of ethanol to their water dispersions. Therefore TGA analysis could not be performed on isolated (precipitated) citrate/phen-capped LaF_3:Eu(5%) NCs. The phen ligand, which is soluble in a range of organic solvents keeps citrate/phen-caped LaF_3:Eu(5%) NCs dispersed upon addition of organic solvents such as ethanol, methanol, acetone and acetonitrile.

Luminescence properties

Luminescence from all (surface and interior) Eu^{3+}-dopant sites of LaF_3:Eu(5%) NCs in water. In an attempt to systematically investigate the luminescence properties Eu^{3+} dopant sites having possibly different local environments in the NCs, we first present the average luminescence behaviour of these dopants, *i.e.,* average emission profile originating from all the dopant sites (surface as well as interior) in the NC matrix. Figure 5 shows the room temperature excitation spectrum, and emission spectra at different excitation wavelengths of citrate-capped LaF_3:Eu(5%) NCs dispersed in water. The excitation spectrum (Figure 5a) was obtained by monitoring the most intense emission line at 616 nm, and various peaks observed in the excitation spectrum are assigned to $^5F_4 \leftarrow {}^7F_0$ (295 nm), $^5H_6 \leftarrow {}^7F_0$ (317 nm), $^5D_4 \leftarrow {}^7F_0$ (361 nm), $^5G_2 \leftarrow {}^7F_0$ (379 nm), $^5L_6 \leftarrow {}^7F_0$ (395 nm), $^5D_3 \leftarrow {}^7F_0$ (413 nm) and $^5D_2 \leftarrow {}^7F_0$ (464 nm) transitions of Eu^{3+} ion.[22] Only f-f transitions of the dopant Eu^{3+}-sites are observed in the excitation spectrum, which means that dopant energy levels are directly populated. Upon excitation of the f-f energy levels of Eu^{3+}-dopant sites at various wavelengths, the NCs display characteristic emission profile of the Eu^{3+} ion, and various emission peaks observed are assigned to $^5D_0 \rightarrow {}^7F_0$ (555 nm); $^5D_0 \rightarrow {}^7F_1$ (592 nm); $^5D_0 \rightarrow {}^7F_2$ (616 nm); $^5D_0 \rightarrow {}^7F_3$ (653 nm); and $^5D_0 \rightarrow {}^7F_4$ (696 nm) transitions of Eu^{3+} ion (Figure 5b). The emission intensity displayed by the NCs at different excitation wavelengths directly corresponds to the intensity displayed by the excitation transitions. Therefore, most intense emission is observed by exciting at 395 nm wavelength which corresponds to the $^5L_6 \leftarrow {}^7F_0$ transition of the Eu^{3+} ion. It is important to note that there are no f-f transitions between 330-350 nm region of the excitation spectrum, and therefore no emission is observed upon excitation at 334, 347 and 350 nm wavelengths.

The integrated intensity ratio of the $^5D_0 \rightarrow {}^7F_2$ electric-dipole transition and $^5D_0 \rightarrow {}^7F_1$ magnetic dipole transition, which is also popularly known as asymmetry ratio (or *R*-value),[23] is used as a sensitive parameter to measure the deviation of local symmetry around Eu^{3+} ion in a lattice site, as well as polarizability of the ligand.[4,7d-f,8a,b,24,25] A higher *R*-value could be carefully associated with lower symmetry around the Eu^{3+} ion,[25] while keeping in mind that highest *R*-values are often displayed europium β-diketonate complexes due to the reasons of high polarizability of the chelating β-diketonate ligands than symetry.[25a] The emission spectra obtained from citrate-capped LaF_3:Eu(5%) NCs dispersed in water at different excitation wavelengths display a similar *R*-value of 1.62, which is consistent with the values obtained in the literature for similar ultra-small (<10 nm) citrate-capped LaF_3:Eu(5%) NCs.[7d,24] It is important to note that upon direct excitation of these NCs, all the dopant sites are excited simultaneously without any discrimination of their spatial location (surface or interior), and the emission spectrum thus observed is an

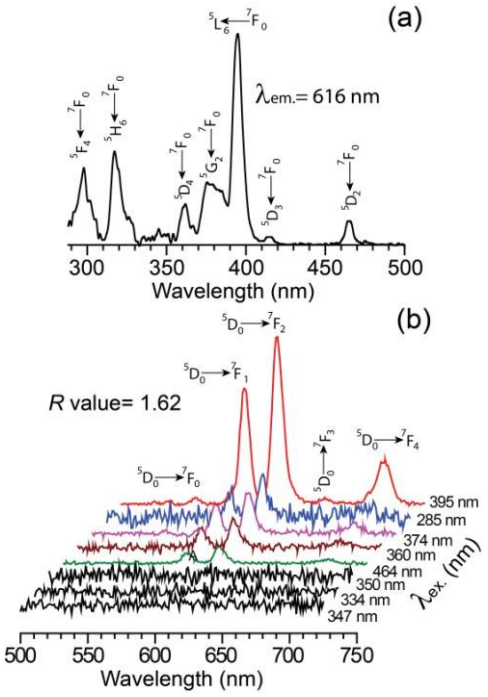

Figure 5. (a) Excitation spectrum and (b) emission spectra at different excitation wavelengths of citrate-capped LaF_3:Eu(5%) NCs dispersed in water, at room temperature. All the emission spectra display a similar *R* value of 1.62. No emission is observed by exciting at 334, 347 and 350 nm wavelengths.

average profile representing dopants with possibly different local environments between surface and interior of the NCs. In LaF_3 matrix of the NCs, the Eu^{3+} dopants are known to occupy La^{3+} sites, and according to a know crystal structure of LaF_3,[26] each La^{3+} has a coordination number of nine and a two-fold axis of symmetry. Since the *R*-values estimated from the emission spectra is an average value of surface dopant sites (coordinated with citrate capping ligands and water molecules, in addition to fluoride ligands) as well as interior dopants (purely coordinated with fluoride ligands), therefore this *R*-value estimated from the spectra cannot be associated with the C_2 site symmetry of the Eu^{3+} dopant sites with a coordination number of 9 in LaF_3 matrix.

Phen sensitized emission from surface Eu^{3+}-dopant sites of LaF_3:Eu(5%) NCs in water. Figure 6 shows the excitation spectrum and emission spectra at two different excitation wavelengths of citrate/phen-capped LaF_3:Eu(5%) NCs dispersed in water, at room temperature. Unlike citrate-only capped LaF_3:Eu(5%) NCs, the excitation spectrum (Figure 6a) of these surface modified NCs (obtained by monitoring the $^5D_0 \rightarrow {}^7F_2$ emission line, at 616 nm) displays a reasonably broad excitation band in the 300–400 nm region. This band is partially overlapped by a moderately intense peak at 395 nm, which is no doubt $^5L_6 \leftarrow {}^7F_0$ transition of the Eu^{3+} ion. Indeed $^5D_2 \leftarrow {}^7F_0$ transition of Eu^{3+} at 464 nm can also be observed in this excitation spectrum. However, the broad excitation band with maxima at 347 nm matches well with the excitation spectrum obtained for free phen in water at room temperature (λ_{max}= 340 nm, Figure S8, ESI†), and therefore is no doubt due to surface-capped phen ligands of these NCs, which confirms that surface capped phen ligands act as sensitizers of the Eu^{3+} dopant emission. The emission spectra of these NCs dispersed in water at two different excitation wavelength, *i.e.,* at 395 nm (corresponding to $^5L_6 \leftarrow {}^7F_0$ transition of the Eu^{3+} ion) and 347 nm (attributed to $\pi\pi^*$ transition of the phen capping ligands) are shown in Figure 6b. The emission spectrum obtained upon 395 nm excitation is similar to the spectrum observed for citrate-only capped LaF_3:Eu(5%) NCs, both furnish a similar *R*-value and indicates that partial replacement of citrate capped ligands by phen does not affect the asymmetry ratio of these NCs.[24] However, the emission spectrum obtained upon 347 nm excitation (*i.e.* excitation of partially-capped phen ligands) shows more intense $^5D_0 \rightarrow {}^7F_2$ transition as compared to the $^5D_0 \rightarrow {}^7F_2$ emission transition obtained by direct excitation (395 nm excitation), and furnishes a higher *R*-value of 2.6. The higher intensity of this emission observed upon 347 nm excitation is a consequence of energy transfer from surface-capped phen ligands after absorption of light, to the $^5D_0$ emitting levels of nearby Eu^{3+} dopant sites. This type of ligand to metal energy transfer (or sensitization) in lanthanide complexes is known to follow a simplified mechanism, in which photons are excited from the lower energy singlet state of the ligand to the higher energy singlet state ($S_0 \rightarrow S_1$), followed by the non-radiative

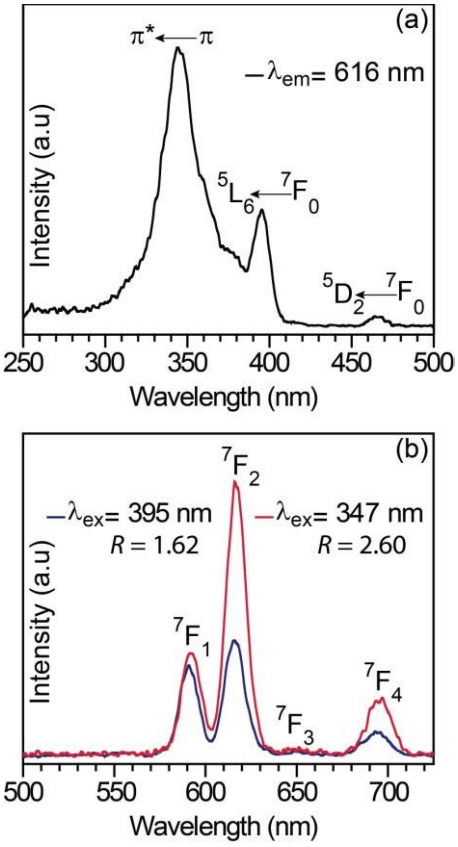

Figure 6. (a) Excitation spectrum and (b) emission spectra at two different excitation wavelengths (395 and 347 nm) of citrate/phen capped LaF3:Eu(5%) nanoparticles dispersed in water, at room temperature. The excitation spectrum has been obtained by monitoring the 616 nm emission ($^5D_0 \rightarrow {}^7F_2$ transition) of the nanoparticles.

intersystem crossing to the triplet state of the ligand ($S_1 \rightarrow T_1$), and finally the energy is mediated via lowest energy triplet state of the organic ligand to the emitting level of the Eu^{3+} ($T_1 \rightarrow {}^5D_0$).[27] The triplet state of the ligand should higher than the emitting level of the Eu^{3+} ion for efficient energy transfer to occur, otherwise non-radiative deactivation occurs via back-energy transfer. Too large gap between the triplet state of the ligand and emitting level of the Ln^{3+} ion also results in poor overlap and therefore poor or no energy transfer. The phen ligand is known to be a good sensitizer of Eu^{3+} ion,[13] because of its near suitable triplet state energy of ~21,500 cm^{-1} with respect to the energy of ${}^5D_0$ emitting level (17,500 cm^{-1}) of Eu^{3+}. The rigidly planar structure of phen also plays an important role in efficiently transferring the energy to the Eu^{3+} ion.[28] The Eu^{3+} ion is very poor in absorbing the light directly because of the Laporte forbidden nature of the f-f transitions. Therefore, the enhancement of emission from LaF_3:Eu(5%) NCs due to sensitization by partially-caped phen ligands, without compromising on their water dispersibility is remarkable, and could be exploited to efficiently image biological samples as compared to direct excitation.

The sensitization of lanthanide emission is well known to be effective over a very short distance between the sensitizer and Ln^{3+} ion.[29] While considering that phen-sensitization of the NCs furnishes a different emission profile as compared to the emission profile obtained upon direct excitation, it can be safely predicted that sensitization by phen ligands would be effective to only surface dopant sites of the NCs in water. In order to confirm this, we have synthesized $[Eu(phen)_2(NO_3)_3]$ complex, and recorded its excitation and emission spectra in the solid state (Figure S11; ESI†). The excitation spectrum of the complex displays a broad band with maxima at 350 nm along with very weak bands due to f-f transitions, similar to that reported in literature for this complex,[13c] which confirms that phen acts as a sensitizer to the Eu^{3+} ion. The emission spectra of the complex upon excitation at 350 nm (corresponding to the ππ* transitions of the phen) and 395 nm (corresponding to ${}^5L_6 \leftarrow {}^7F_0$ transition of the Eu^{3+} ion) show similar emission profiles (*R*-value = 7.8), unlike the emission spectra of citrate/phen-capped LaF_3:Eu(5%) NCs which display different emission profiles upon excitations at 347 and 395 nm wavelengths (Figure 6). This is observed due to similar local environment of Eu^{3+} centre in $[Eu(phen)_2(NO_3)_3]$ complexes. Thus, a comparative study of PL excitation and emission spectra of citrate/phen-capped LaF_3:Eu(5%) NCs and $[Eu(phen)_2(NO_3)_3]$ complex, in which only phen acts as a sensitizer in both materials reveals that phen sensitizes only surface Eu^{3+} dopant sites of the NCs in water, which have different local environment as compared to the interior Eu^{3+} dopant sites. Therefore, partially surface capping phen ligands while acting as sensitizers for Eu^{3+} sites, also act as probes and allow us to differentiate between emission profile of surface dopant sites from the average emission profile of surface and interior dopant sites. The higher *R*-value estimated from the emission spectrum upon excitation of surface capping phen ligand is consistent with the observations reported in the literature on surface sensitized Eu^{3+}-doped nanoparticles in various matrices.[7c-g,8a] The higher *R*-value suggests that the Eu^{3+} local environment of the surface dopant sites is different as compared to the average environment of all the dopant sites in the NCs, which could be either attributed to increase in the asymmetry around these surface dopant sites by phen capping ligands,[24] or to higher polarizability of the surface chelating phen ligands as compared to fluorine ligands.[25] However, it is generally believed that the capping ligands introduce symmetry distortion to the surface dopant sites due to which the *R*-value of surface dopant sites is increased as compared to interior sites.[7d-f,8a,24]

Time-gated (or time-resolved) emission spectroscopy

In order to fully realize the potential applications of Ln-doped nanoparticles in optoelectronics and bioscience, we believe it is important to have a detailed understanding of the luminescence properties of different Ln^{3+}-dopant sites. There are very few reports available in the existing literature in which the luminescence properties of different Ln^{3+}-dopant sites (*i.e.,* surface and interior sites) of Ln-doped nanoparticles have been investigated thoroughly while using techniques such as site-selective spectroscopy.[30] TRES is an important technique which can also be used to study the PL dynamics of different Ln^{3+}-sites of Ln-doped NCs.[4] In this work, since we can excite all the Eu^{3+} sites of the LaF_3:Eu(5%) NCs via direct excitation, as well as selectively excite surface Eu^{3+}-sites of the NCs via sensitization by phen ligands, therefore TRES of these NCs using two different excitation wavelengths could be very helpful in understanding the PL dynamics of different Eu^{3+}-sites of these NCs.

TRES of LaF_3:Eu(5%) NCs upon direct excitation. Figure 7a shows a TRES plot of the citrate-capped LaF_3:Eu(5%) NCs dispersed in water, and collected over a period of several milliseconds (delays between 0.1 ms-24.5 ms; fixed gate-time of 2 ms; $\lambda_{ex.}$= 395 nm) at room temperature. The emission spectra of the NCs display a steady decrease in intensity at successive delay-times until 25 ms delay, beyond which no emission is observed. Considering the magnetic- and electric-dipole nature of the ${}^5D_0 \rightarrow {}^7F_1$ (592 nm) and ${}^5D_0 \rightarrow {}^7F_2$ (616 nm) emission transitions,[31] respectively, we monitored the emission intensity decay of both the transitions with respect to delay time. The time-resolved emission intensity decay plot of the ${}^5D_0 \rightarrow {}^7F_1$ magnetic-dipole transition at 592 nm is shown in Figure 7b, which could be best fit to a tri-exponential curve. The average PL lifetime of the Eu^{3+}-dopant emission obtained by monitoring the ${}^5D_0 \rightarrow {}^7F_1$ emission decay is 4.17 ms, which is slightly higher than the lifetime ($\tau_{av.}$= 0.33 ms; $\lambda_{ex.}$= 396 nm, $\lambda_{em.}$= 590 nm) reported recently for a similar oleylamine-capped LaF_3:Eu nanoparticles dispersed in polydimethylsiloxane.[32] The three time constants, τ_1, τ_2 and τ_3, obtained from the tri-exponential fit of the ${}^5D_0 \rightarrow {}^7F_1$ emission decay could be attributed to at least three different types of Eu^{3+} emitting sites of the NCs. The longest lifetime component, "τ_1" (τ_1 = 7.04 ms) having the largest contribution (48.48%) is safely be attributed to Eu^{3+} dopant sites from in the interior of the NCs. These dopant sites are very well protected from vibrational quenching of the citrate capping ligands and surrounding aqueous environment. The other lifetime

View Article Online
DOI: 10.1039/C6DT01917J

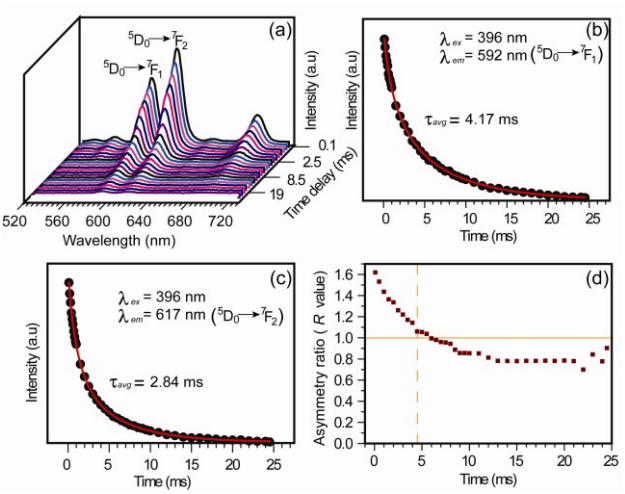

Figure 7. (a) Time-resolved emission spectra of citrated-capped LaF_3:Eu(5%) NCs dispersed in water, at room temperature. The spectra were recorded with a fixed gate-time of 2 ms, and different delay times from 0.1-24.5 ms, beyond which no emission is observed; (b, c) PL decay curves (black dots) and tri-exponential fit (red lines) of the Eu^{3+} emission obtained by monitoring the integrated emission intensity of $^5D_0 \rightarrow {}^7F_1$ (592 nm) and $^5D_0 \rightarrow {}^7F_2$ (616 nm) transitions, respectively, with time; (d) Plot of *R* values monitored with delay-time. The horizontal (solid line) and vertical (dashed line) have been drawn to depict time and *R* value where intensity of $^7F_1$ and $^7F_2$ emission line is similar.

components (τ_2 and τ_3) which have a very short lifetime as compared to τ_1, could be attributed to the surface or near surface dopant sites. Among them, the lifetime component "τ_3'' (τ_3= 0.4 ms, 13.75%) with least abundance is safely be attributed to Eu^{3+} dopant sites which are in direct coordination with capping-ligands and surrounding water molecules, and thereby most affected by vibrational quenching of –OH oscillators.[33] The lifetime component "τ_2'' (τ_2= 1.85 ms, 37.76%) is attributed to dopant sites which are not completely protected from the vibrational quenching of the capping ligands and surrounding water molecules. These dopant sites are possibly close to the surface (few coordinating shells below the surface) because they have much longer lifetime than dopant sites attributed to purely to the surface of the NCs. The time-resolved emission intensity decay plot of the $^5D_0 \rightarrow {}^7F_2$ electric-dipole transition at 617 nm is shown in Figure 7c, which could also be best fit to a tri-exponential curve. Strikingly, the average lifetime obtained from the $^5D_0 \rightarrow {}^7F_2$ emission decay (2.84 ms) is much lower than the lifetime obtained from the $^5D_0 \rightarrow {}^7F_1$ emission decay. The three time constants obtained from the tri-exponential fit of the $^5D_0 \rightarrow {}^7F_2$ emission decay show similar distribution as obtained from $^5D_0 \rightarrow {}^7F_1$ emission decay. However, the slowest component attributed to the interior dopant sites has lower lifetime (5.5 ms), as compared to $^5D_0 \rightarrow {}^7F_1$ emission lifetime of the interior dopant sites. The other two components display lifetime values of 1.33 ms and 0.32 ms, which are attributed to near-surface and purely surface dopant sites of the NCs, as explained for the $^5D_0 \rightarrow {}^7F_1$ emission decay components.

A significant variation in the average lifetimes of the citrate-stabilized LaF_3:Eu(5%) NCs dispersed in water at 592 and 616 nm emissions suggests that their relative intensity is

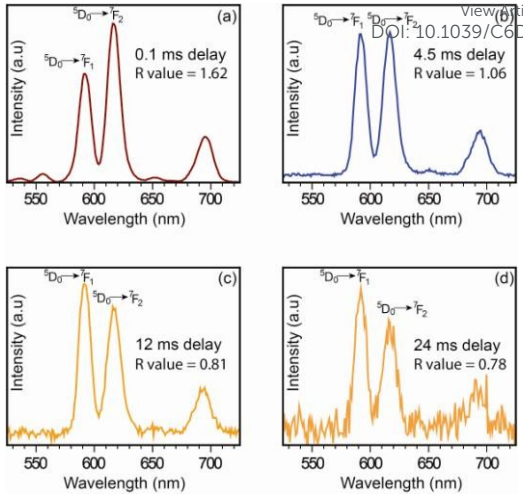

Figure 8. Representative emission spectra of citrated-capped LaF_3:Eu(5%) NCs collected at (a) 0.1 ms; (b) 4.5 ms; (c) 12.0 ms and (d) 24.0 ms delay times, depicting variation in the relative emission intensities of $^5D_0 \rightarrow {}^7F_2$ and $^5D_0 \rightarrow {}^7F_1$ emission transitions (or *R* values).

highly sensitive to the local environment, which could be further probed by estimating the *R*-values of the time-resolved emission spectra.[4,34] Figure 7d shows a plot of the *R*-values estimated from the TRES profiles at different delay times. The *R*-values can be observed to decrease rapidly from the value of 1.62 at 0.1 ms delay time until the value of ~1 at 5 ms delay time. The *R*-values show further slow decrease up to 12 ms delay to a value of ~0.8, and beyond which it remains almost same. The representative TRES spectra shown in Figure 8 clearly show three distinct emission profiles of Eu^{3+} dopant sites of the NCs at different delay times, and corroborates well with the results of triexponential decay. However, these emission profiles cannot be attributed to purely three different dopant sites of the NCs.

These distinct emission profiles at different delay times are interpreted with the help of three different lifetime components obtained from triexponential decay. The time-resolved emission spectra obtained after initial time-delays (possibly up to ~5 ms delay-time) are attributed to be representative of all the three different dopant sites in these NCs, but the contribution of surface sites would decrease rapidly at successive delay time due to their fast decay (τ < 0.4 ms for both transitions). Further, we have observed that the surface sites have higher *R*-values (as found with phen sensitization) possibly due to symmetry distortion introduced by capping ligands,[24] and therefore as the contribution of surface dopant emission vanish in the TRES profiles of these NCs (at successive delay times), the emission profiles of less distorted near-surface and interior sites would dominate, and that is possibly the reason we also see much rapid decrease in the *R*-values of the initial delay times. After ~5 ms delay-time, the TRES profiles of the NCs are expected to have contributions from near-surface dopants as well as purely interior dopants, because surface dopants which are in direct contact with citrate ligands and surrounding water molecules are expected to have completely decayed up to this time. Beyond ~5 ms time-delays, the contribution of near surface

dopant sites will also decrease rapidly from the TRES profiles, and we believe their decay would be complete up to around 12 ms delay time. There is a slow decrease in the *R*-values in this time regime (5-12 ms), which is possibly because there is very less deviation in the asymmetry of near-surface dopant sites as compared to the interior sites. From 12 ms delay-time up to 24.5 ms delay-time beyond which no emission is observed, all TRES profiles are similar and the *R*-values estimated from them also display a similar value. We have no doubt that these are the time-resolved emission profiles of purely interior Eu^{3+} dopant sites of LaF_3:Eu(5%) NCs, because of their long PL lifetime. These emission profiles and their *R*-values (0.8 ± 0.02) can be associated with the C_2 site symmetry of the Eu^{3+} dopant sites, with a coordination number of 9 in LaF_3 matrix.[26]

TRES of LaF_3:Eu(5%) NCs upon sensitization by phen ligands. Figure 9a shows a TRES plot (delays between 0.1 ms-1.0 ms; fixed gate-time of 2 ms; $\lambda_{ex.}$= 347 nm) of the citrate/phen-capped LaF_3:Eu(5%) NCs dispersed in water at room temperature. No time-resolved emission is observed beyond 1 ms time-delay. The time-resolved emission intensity decay curves obtained by monitoring $^5D_0 \rightarrow {}^7F_1$ magnetic-dipole transition at 592 nm and $^5D_0 \rightarrow {}^7F_2$ electric-dipole transition at 616 nm, are shown in Figure 9b and c, respectively, both of which could be best fit to mono-exponential decay. The lifetime of phen-sensitized europium emission obtained from these NCs in water by monitoring $^5D_0 \rightarrow {}^7F_1$ (592 nm) as well as $^5D_0 \rightarrow {}^7F_2$ (616 nm) emission transitions is strikingly similar (*i.e.,* τ= 0.27 ms), unlike the different lifetimes obtained by monitoring these emission transitions upon direct excitation of the NCs. The sensitized europium emission lifetimes observed

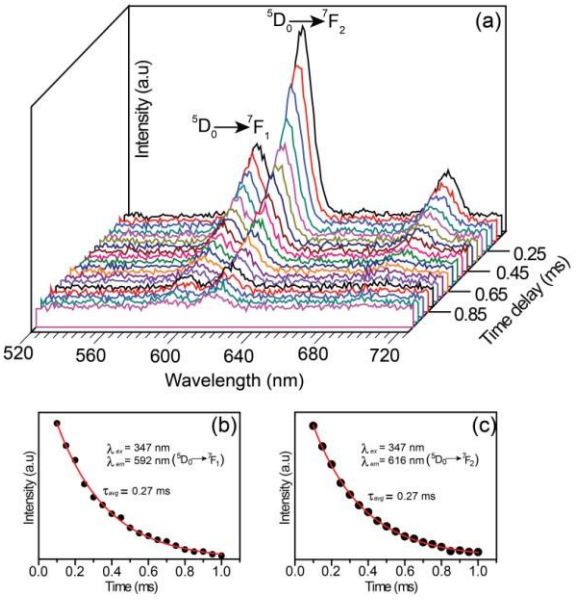

Figure 9. (a) Time-resolved emission spectra of citrated/phen-capped LaF_3:Eu(5%) NCs dispersed in water, at room temperature, collected with a fixed gate-time of 2 ms and different delay times from 0.1-1.0 ms, beyond which no emission is observed; (b, c) PL decay curves (black dots) and mono-exponential fit (red lines) of the Eu^{3+} emission obtained by monitoring the integrated emission intensity of $^5D_0 \rightarrow {}^7F_1$ (592 nm) and $^5D_0 \rightarrow {}^7F_2$ (616 nm) transitions, respectively, with time.

in aqueous solutions are usually in the range of 0.1-1.2 ms,[35] and these lower lifetimes arise because of energy transfer process from metal excited states to the –OH stretching vibrations of the coordinated or closely diffusing water molecules.[33,35a] The lower value of phen-sensitized PL lifetime of Eu^{3+} dopant sites therefore suggests that –OH and –CH oscillators of the citrate capping ligands and water molecules near these surface sites are responsible for the non-radiative deactivation of the sensitized emission from Eu^{3+} excited states. However, the observed lifetime of the phen-sensitized europium emission in these NCs is remarkably similar to the lifetime reported by Bunzli and co-workers for $[EuCl_2Phen_1(H_2O)_4]Cl_1(H_2O)$ complex in the solid state, in which europium ion is coordinated with one phen sensitizer.[13b] In the same report,[13b] the lifetimes of $[EuCl_1Phen_2(H_2O)_3]Cl_2(H_2O)$ and $[EuCl_2Phen_2(H_2O)_2]Cl_1(H_2O)$ complexes in the solid state, in which europium ions in each complex are coordinated with two phen sensitizer are 0.30 and 0.38 ms, respectively which are slightly higher than the lifetime of phen-sensitized emission in LaF_3:Eu(5%) NCs in water. It is remarkable that the lifetimes of the phen-sensitized emission in these solid state complexes are comparable to the lifetime observed for phen-sensitized emission from LaF_3:Eu(5%) NCs dispersed in water. These observations point out that the strategy of protecting the dopants in the NC host from non- radiative deactivation via high-energy vibrations of the solvent molecules and capping ligands, combined with sensitization of these dopant sites by surface capped organic chromophores,[7a] can produce efficient emission even in water dispersible Ln-doped nanoparticles. Indeed, similar observations have also been noted very recently by Charbonnière and coworkers in their study on Tb-doped nanoparticles.[8c] Further, we note that the PL lifetime observed from Eu^{3+} dopant sites upon sensitization by phen ligands in water is much higher than the lifetime reported from 6-carboxy-5′-methyl-2,2′ -bipyridine ($bipyCOO^-$) sensitized LaF_3:Eu(5%) nanopartticles in water (τ= 0.125 ms).[7c] This indicates that phen is an efficient surface sensitizer for Eu^{3+} dopant sites in LaF_3 NC matrix in water as compared to $bipyCOO^-$.

The monoexponential lifetime decay of the phen-sensitized Eu^{3+} dopant emission, and their very lower lifetime as compared to the lifetime constants obtained for near surface and interior Eu^{3+} sites of the LaF_3:Eu(5%) NCs (upon direct excitation) reveals that phen truly sensitizes purely surface Eu^{3+} sites in aqueous medium. The reason being that the possible sensitization of near surface Eu^{3+} sites of these NCs, which are more protected from non-radiative deactivation by –OH oscillators is expected to produce much higher lifetime and a multiexponential decay.[7g,8a] The sensitization of purely surface Eu^{3+} sites of the LaF_3:Eu(5%) NCs by phen is further demonstrated by the *R*-values evaluated from the time-gated emission profiles of the phen sensitized Eu^{3+} dopant emission (Figure 10a), which remain constant (2.4±0.2) within the errors of the integration of the emission peaks at successive delay times. The *R*-values in general have been well established to display a significant change upon change in the local environment around Eu^{3+} sites in the nanoparticles.[24,34]

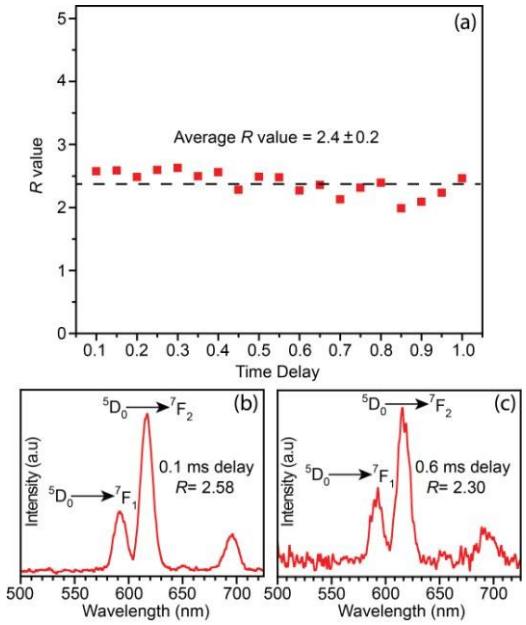

Figure 10. (a) Plot of *R*-values monitored with delay-times for the time-gated emission spectra of citrated/phen-capped LaF_3:Eu(5%) NCs dispersed in water and obtained upon 347 nm excitation, at room temperature. The horizontal (dashed line) has been drawn to depict average *R* value obtained from various time-gated emission spectra. (b,c) Representative time-gated emission spectra of citrated/phen-capped LaF_3:Eu(5%) NCs at 0.1 and 0.6 ms delay times, depicting negligible variations in the relative emission intensities of $^5D_0 \rightarrow {}^7F_2$ and $^5D_0 \rightarrow {}^7F_1$ emission transitions.

Further, the *R*-values of the time-gated spectra provide a detailed insight of the PL dynamics of the Eu^{3+} in different coordinating sites, i.e. surface and interior dopants.[4,8a] Therefore, a consistent value of the different time-gated emission spectra reveals that the local environment around all the Eu^{3+} sites sensitized by phen is nearly similar. The representative time-gated emission spectra obtained at 0.1 and 0.6 ms delay times are shown in Figure 10b and c, which appear as similar profiles (change in *R*-value is ±0.2), and therefore are attributed to purely surface dopant sites of the citrate/phen-capped LaF_3:Eu(5%) NCs.

Assessment of phen–sensitized Eu^{3+}-emission stability of the NCs in presence various buffers and organic solvents. Luminescent water soluble nanomaterials find potential applications in biological imaging of cells. The cells possess a buffered environment that effectively maintains their physiological pH. Here we present a model study on the luminescence properties of citrate/phen-capped LaF_3:Eu(5%) NCs in a buffered environment with a view to assess their suitability for development as emissive probes. We have selected three biological buffers such as 4-(2-hydroxyethyl)-1-piperazineethanessulfonic acid (HEPES-buffer), tris(hydroxymethyl)aminomethane (Tris-buffer) and phosphate-buffer, which are often used to mimic the buffering activity of the cells, to assess the effect of these buffer systems on phen-sensitized luminescence of the NCs. In these experiments, 3 mM stock solutions of HEPES-buffer, Tris-buffer and phosphate-buffer at physiological pH (7.4) were prepared in water and mixed in 1:1 v/v ratio with water dispersions of citrate/phen-capped LaF_3:Eu(5%) NCs (conc. ~8 mg/mL). Figure 11a shows the effect of different buffer solutions on phen-sensitized Eu^{3+}-emission upon addition with NC dispersions in water (1:1 v/v ratio). Upon excitation at 347 nm, the emission intensity remains almost unchanged by addition of Tris-buffer as compared to Eu^{3+} emission intensity in water without any buffer. However, the addition of HEPES and phosphate-buffer moderately increases the intensity. Further, the relative intensity of the same samples measured over a period of 36 hours remains almost unperturbed. The modest increase in sensitized Eu^{3+} emission in presence of phosphate and HEPES suggests that these buffers interact with the NC surface and partially replace the aqueous environment around the surface dopant sites which results in reducing the quenching of Eu^{3+} emission by –OH oscillators of water.

The partial replacement of water molecules on the surface of the NCs resulting in enhancement of phen-sensitized Eu^{3+} luminescence has been further confirmed by a series of experiments undertaken on these NCs with organic solvents. Four water-miscible organic solvents (methanol, ethanol, acetone and acetonitrile) were mixed in 1:1 v/v ratio with water dispersions of citrate/phen-capped LaF_3:Eu(5%) NCs (conc. ~8 mg/mL). Figure 11b shows the effect of addition of water-miscible organic solvents on the phen-sensitized

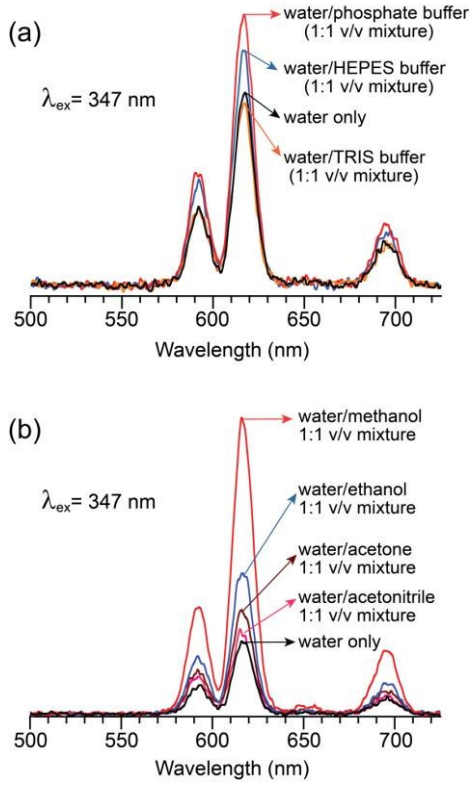

Figure 11. (a) Emission spectra citrate/phen-capped LaF_3:Eu(5%) NCs in a 1:1 v/v mixture of water and various buffers (phosphate-buffer, HEPES-buffer and Tris-buffer) at physiological pH (7.4). (b) Emission spectra of citrate/phen-capped LaF_3:Eu(5%) NCs in a 1:1 v/v mixture of water and various water-miscible solvents (methanol, ethanol, acetone and acetonitrile).

luminescence intensity of the NCs. Upon excitation at 347 nm, the addition of methanol strikingly enhances the luminescence intensity of the NCs, followed by modest enhancement upon addition of ethanol. The addition of acetone and acetonitrile does not enhance the luminescence intensity significantly. Among these solvents, methanol is a strongly coordinating solvent, and therefore is expected to replace significant number of water molecules on the surface of these NCs and decrease the influence of quenching of Eu^{3+} emission by –OH oscillators of water. The relative intensity of the samples containing organic solvents measured over a period of 36 hours remains almost unperturbed.

Two-photon excited PL imaging of citrate/phen-capped LaF_3:Eu(5%) NC aggregates. Imaging of biological samples using luminescent lanthanide complexes and lanthanide-doped nanoparticles often needs UV excitation, which could be harmful for biological imaging.[36] The use of UV light can be avoided by two-photon excitation, in which the sample concurrently absorbs two higher wavelength photons (of equal energy), and subsequently produces the emission of a lower wavelength photon.[36a,37] This microscopy technique has become very popular in recent years in which the sample is excited with wavelengths located in the biologically transparent near infrared (700-900 nm) spectral region, and therefore allows deeper penetration of the biological samples and reduces photobleaching.[38] Figure 12 shows the two-photon excited PL images of citrate/phen-capped LaF_3:Eu(5%) NC aggregates formed by drop casting the sample from an aqueous dispersion on a silica coverslip. These images were taken from the same area of the sample using two different two-photon excitation wavelengths (*i.e.* 720 and 790 nm), both having same power (*i.e.* excitation power of 60 mW was used for imaging an area of 134.8 x134.8 μm^2 area). The PL image obtained by exciting the NC aggregates using 790 nm two-photon wavelength (Figure 12a), which corresponds to the wavelength doubled one photon excitation of the $^5L_6 \leftarrow {}^7F_0$ transition (395 nm) of the Eu^{3+} ions does not produce any emission from the aggregates at such a low power of the laser. However, upon excitation of the same area of NC aggregates with 720 nm two-photon wavelength (Figure 12b), which simultaneously corresponds to the wavelength doubled one photon excitation band of the phen capping-ligands (see Figure 6a for reference) as well one photon excitation of $^5D_4 \leftarrow {}^7F_0$ transition (360 nm) of Eu^{3+}, the NC aggregates produce a very bright red emission at such a low power of laser. These preliminary results reveal that water dispersed citrate/phen-capped LaF_3:Eu(5%) NCs could be suitable for imaging biological samples under two-photon excitation, which is currently being explored.

Conclusions

In summary, we have demonstrated that LaF_3:Eu NCs which are water dispersible due to citrate capping ligands, undergo partial ligand-exchange with neutral nitrogen donor phen ligands in aqueous medium at moderate temperature while retaining their water dispersibility. This synthetic strategy

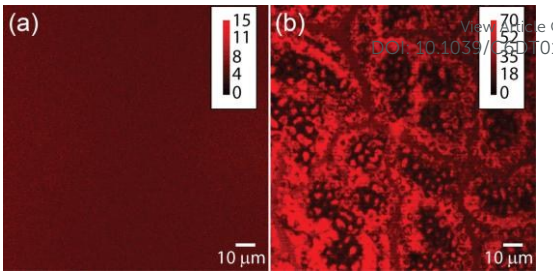

Figure 12. Two-photon excited PL images of citrate/phen capped LaF_3:Eu(5%) NC aggregates caste on a silica substrate and excited with (a) 790 nm and (b) 720 nm two-photon wavelengths. The images were taken on a Carl Zeiss LSM-780 confocal microscope equipped with a two photon coherent chameleon pulsed Ti:sapphire laser. The emission was collected using 594-668 nm filter.

affords a general platform to partially functionalize the surfaces of water-soluble Ln^{3+}-doped nanoparticles containing non-sensitizing capping ligands, with those NN donor sensitizing ligands which are weakly soluble in water at room temperature. The partially surface-capped phen ligands of the resulting NCs dispersed in water act as sensitizers of the surface dopants, which results in a significant enhancement of luminescence intensity from these NCs in water as compared to direct excitation of the dopant energy levels. The time-gated emission spectroscopy of the LaF_3:Eu NCs upon direct excitation reveals that Eu^{3+} dopants occupy at least three different sites in the NC matrix. The purely interior dopant sites of the NCs which are well protected from quenching by –OH and –CH oscillators of the capping ligands and nearby water molecules display much higher lifetime as compared purely surface and near surface sites, and their emission profile could be resolved by time-gated emission spectroscopy. The time-gated emission spectra obtained from citrate/phen-capped LaF_3:Eu(5%) NCs upon excitation of phen ligands further reveals that phen-sensitized emission from the NCs is displayed by purely surface dopant sites. The efficiency of the phen-sensitized emission observed from LaF_3:Eu NCs is noteworthy, which is proved by its significantly large lifetime in water. The phen-sensitized Eu^{3+} emission of the NCs remains stable over a long period of time in pure water, as well as in presence of biological buffers at physiological pH and organic solvents. The excitation of the citrate/phen-capped LaF_3:Eu(5%) NC aggregates upon 720 nm two-photon wavelength produces a bright red emission, which could be useful for imaging biological samples. The two photon imaging of various biological cells using citrate/phen-capped LaF_3:Eu(5%) is currently under investigation.

Acknowledgements

A.C acknowledges IRCC, IIT Bombay for funding. M.I acknowledges Science and Engineering Research Board (SERB), Department of Science and Technology (Govt. Of India) for financial grant under the scheme “Start-Up Research Grant (Young Scientists)”, no. SB/FT/CS-098/2013. We thank Professors Anindya Datta and Naresh Patwari for helping with time resolved photoluminescence measurements, critical comments and valuable discussions.

Notes and references

1 (a) C. Lorbeer, J. Cybinska and A.-V. Mudring, *J. Mater. Chem. C,* 2014, ***2***, 1862-1868; (b) S. Wu, G. Han, D. J. Milliron, S. Aloni, V. Altoe, D. V. Talapin, B. E. Cohen and P. J. Schuck, *Proc. Natl. Acad. Sci. USA,* 2009, ***106***, 10917–10921; (c) A. D. Ostrowski, E. M. Chan, D. J. Gargas, E. M. Katz, G. Han, P. J. Schuck, D. J. Milliron and Bruce E. Cohen, *ACS Nano*, 2012, ***6***, 2686–2692; (d) W. Niu, S. Wu, S. Zhang and L. Li, *Chem. Commun.,* 2010, ***46***, 3908–3910; (e) F. Wang, Xiaogang Liu, *Acc. Chem. Res.,* 2014, ***47***, 1378−1385.

2 (a) Y. Liu, D. Tu,a H. Zhu and X. Chen, *Chem. Soc. Rev.,* 2013, ***42***, 6924-6958; (b) S. Zheng, W. Chen, D. Tan, J. Zhou, Q. Guo, W. Jiang, C. Xu, X. Liu and J. Qiu, *Nanoscale*, 2014, ***6***, 5675–5679; (c) G. Wang, Q. Peng, and Y. Li, *Acc. Chem. Res.,* 2011, ***44***, 322-334; (d) X. Huang, S. Han, W. Huang and X. Liu, *Chem. Soc. Rev.,* 2013, ***42***, 173-201.

3 E. Beaurepaire, V. Buissette, M. P. Sauviat, D. Giaume, K. Lahlil, A. Mercuri, D. Casanova, A. Huignard, J. L. Martin, T. Gacoin, J. P. Boilot and A. Alexandrou, *Nano Lett.,* 2004, ***4,*** 2079–2083.

4 T. Wang, A. Layek, I. D. Hosein, V. Chirmanov and P. V. Radovanovic, *J. Mater. Chem. C,* 2014, ***2,*** 3212-3222.

5 (a) Y. Q. Lu, J. Lu, J. B. Zhao, J. Cusido, F. M. Raymo, J. L. Yuan, S. Yang, R. C. Leif, Y. J. Huo, J. A. Piper, J. Paul Robinson, E. M. Goldys and D. Y. Jin, *Nat. Commun.,* 2014, ***5***, 3741; (b) J. Zhao, Z. Lu, Y. Yin, C. McRae, J. A. Piper, J. M. Dawes, D. Jin and E. M. Goldys, *Nanoscale,* 2013, ***5***, 944–952.

6 (a) B. Chen, D. Peng, X. Chen, X. Qiao, X. Fan and F. Wang, *Angew. Chem. Int. Ed.,* 2015, ***54***, 12788 –12790; (b) F. Wang, Y. Han, C. S. Lim, Y. H. Lu, J. Wang, J. Xu, H. Y. Chen, C. Zhang, M. H. Hong and X. G. Liu, *Nature,* 2010, ***463***, 1061–1065; (c) J. H. Zeng, J. Su, Z. H. Li, R. X. Yan and Y. D. Li, *Adv. Mater.,* 2005, ***17***, 2119–2123; (d) L. Wang and Y. Li, *Chem. Mater.,* 2007, ***19***, 727–734.

7 (a) J. Zhang, C. M. Shade, D. A. Chengelis and S. Petoud, *J. Am. Chem. Soc.,* 2007, ***129***, 14834 –14835; (b) B. Kokuoz, J. R. DiMaio, C. J. Kucera, D. D. Evanoff Jr. and J. Ballato, *J. Am. Chem. Soc.,* 2008, ***130***, 12222-12223; (c) L. J. Charbonnière, J.-L. Rehspringer, R. Ziessel and Y. Zimmermann, *New J. Chem.,* 2008, ***32***, 1055-1059; (d) A. M. Cross, P. S. May, F. C. J. M. van Veggel and M. T. Berry, *J. Phys. Chem. C,* 2010, ***114***, 14740-14747; (e) S. Li, X. Zhang, Z. Hou, Z. Cheng, P. Ma and J. Lin, *Nanoscale,* 2012, ***4,*** 5619-5626; (f) J. Chen, Q. Meng, P. S. May, M. T. Berry and C. Lin, *J. Phys. Chem. C,* 2013, ***117***, 5953-5962; (g) S. Janssens, G. V. M. Williams, D. Clarke and M. Sharp, S. Janssens, G. V. M. Williams and D. Clarke, J. *Appl. Phys.,* 2011, ***109***, 023506.

8 (a) M. Irfanullah, D. K. Sharma, R. Chulliyil and A. Chowdhury, *Dalton Trans.,* 2015, ***44***, 3082-3091; (b) M. E. Foley, R. W. Meulenberg, J. R. McBride, and G. F. Strouse, *Chem. Mater.,* 2015, ***27***, 8362−8374; (c) J. Goetz, A. Nonat, A. Diallo, M. Sy, I. Sera, A. Lecointre, C. Lefevre, C. F. Chan, K.-L. Wong, and L. J. Charbonnière, *ChemPlusChem,* 2016, ***81***, 526-534.

9 M. Back, R. Marin, M. Franceschin, N. S. Hancha, F. Enrichi, E. Trave and S. Polizzi, *J. Mater. Chem. C,* 2016, 4, 1906-1913.

10 (a) N. M. Shavaleev, S. V. Eliseeva, R. Scopelliti and J.-C. G. Bunzli, *Inorg. Chem.,* 2014, ***53***, 5171−5178; (b) K. S. Kumar, B. Schäfer, S. Lebedkin, L. Karmazin, M. M. Kappesb and M. Ruben, *Dalton Trans.,* 2015, ***44***, 15611–15619.

11 G. Accorsi, A. Listorti, K. Yoosaf and N. Armaroli, *Chem. Soc. Rev.,* 2009, ***38***, 1690–1700.

12 A. A. Khan and K. Iftikhar, *Polyhedron,* 1994, ***13***, 3199-3208.

13 (a) H. J. Zhang, L.S. Fu, S.B. Wang, Q. G. Meng, K.Y. Yang and J. Z. Ni, *Mater. Lett.,* 1999, ***38***, 260–264; (b) L. N. Puntus, K. A. Lyssenko, M. Y. Antipin and J.-C. G. Bünzli, *Inorg. Chem.,* 2008, ***47***, 11095-11107; (c) T.-H. Yang, L. Fu, R. A. S. Ferreira, M. M. Nolasco, J. Rocha, L. D. Carlos and F.-N. Shi, *Eur. J. Inorg. Chem.,* 2015, 4861–4868; (d) Z. Pan, G. Jia, C.-K. Duan, W.-Y. Wong, W.-T. Wong and P. A. Tanner, *Eur. J. Inorg. Chem.,* 2011, 637–646; (e) S. Quici, M. Cavazzini, G. Marzanni, G. Accorsi, N. Armaroli, B. Ventura and F. Barigelletti, *Inorg. Chem.,* 2005, ***44***, 529-537; (f) S. I. Klink, G. A. Hebbink, L. Grave, P. G. B. O. Alink and F. C. J. M. van Veggel*, J. Phys. Chem. A,* 2002, ***106***, 3681-3689.

14 J. Burgess and R. I. Haines, *J. Chem. Eng. Data.,* 1978, ***23***, 196-197.

15 J.-S. Kang, Y.-K. Jeong, J.-G. Kang, L. Zhao, Y. Sohn, D. Pradhan and K. T. Leung, *J. Phys. Chem. C,* 2015, ***119***, 2142-2147.

16 C. Lorbeer and A.-V. Mudring, *J. Phys. Chem. C,* 2013, ***117***, 12229−12238.

17 (a) C. Dong, J. Pichaandi, T. Regier and F. C. J. M. van Veggel , *Nanoscale*, 2011, ***3***, 3376-3384; (b) F. Li, C. Li, X. Liu, T. Bai, W. Dong, X. Zhang, Z. Shi and S. Feng, *Dalton Trans.,* 2013, ***42***, 2015–2022.

18 (a) Z. L. Wang, Z. W. Quan, P. Y. Jia, C. K. Lin, Y. Luo, Y. Chen, J. Fang, W. Zhou, C. J. O'Connor, and J. Lin, *Chem. Mater.,* 2006, ***18***, 2030-2037; (b) F. Wang, Y. Zhang, X. Fanc and M. Wang, *J. Mater. Chem.,* 2006, ***16***, 1031–1034.

19 M. M. Lezhnina, T. Jüstel, H. Kätker, D. U. Wiechert and U. H. Kynast, *Adv. Funct. Mater.,* 2006, ***16***, 935-942.

20 J. R. DiMaio, B. Kokuoz and J. Ballato, *J. Am. Chem. Soc.,* 2008, ***130***, 5628-5629.

21 (a) V. Sudarsan, S. Sivakumar and F. C. J. M. van Veggel, *Chem. Mater.*, 2005, ***17***, 4736-4742; (b) J. W. Stouwdam and F. C. J. M. van Veggel, *Langmuir,* 2004, ***20***, 11763-11771.

22 W. T. Carnall, P. R. Fields and K. Rajnak, *J. Chem. Phys.*, 1968, ***49***, 4450-4455.

23 H. Nabika and S. Deki, *J. Phys. Chem. B,* 2003, ***107***, 9161-1964.

24 V. Sudarsan, F. C. J. M. van Veggel, R. A. Herring and M. Raudsepp, *J. Mater. Chem.,* 2005, ***15***, 1332–1342.

25 K. Binnemans, Coord. *Chem. Rev.,* 2015, ***295***, 1-45; (b) P. A. Tanner, *Chem. Soc. Rev.,* 2013, ***42***, 5090—5101.

26 A. Zalkin, D. H. Templeton and T. E. Hopkins, *Inorg. Chem.*, 1966, ***5,*** 1466–1468.

27 M. D. Regulacio, M. H. Pablico, J. A. Vasquez, P. N. Myers, S. Gentry, M. Prushan, S.-W. T.-Chang and S. L. Stoll, *Inorg. Chem.,* 2008, ***47***, 1512-1523.

28 M. Irfanullah and K. Iftikhar, *J. Fluoresc.,* 2011, ***21***, 81–93.

29 (a) D. L. Dexter, *J. Chem. Phys.*, 1953, ***21***, 836-850; (b) T. Forster, *Discuss. Faraday Soc.*, 1959, ***27***, 7-17; (c) J.-C. G. Bünzli and C. Piguet, *Chem. Soc. Rev.*, 2005, ***34,*** 1048-1077.

30 (a) O. Lehmann, K. Kömpe and M. Haase, *J. Am. Chem. Soc.,* 2004, ***126***, 14935-14942; (b) C. H. Yan, L. D. Sun, C. S. Liao, Y. X. Zhang, Y. Q. Lu, S. H. Huang and S. Z. Lu, *Appl. Phys. Lett.,* 2003, ***82***, 3511–3513.

31 F. S. Richardson, *Chem. Rev.,* 1982, ***82***, 541-552.

32 E. M. Rodrigues, R. D. L. Gaspar, I. O. Mazali and F. A. Sigoli, *J. Mater. Chem. C,* 2015, ***3,*** 6376-6388.

33 A. Beeby, I. M. Clarkson, R. S. Dickins, S. Faulkner, D. Parker, L. Royle, A. S. de Sousa, J. A. G. Williams and M. Woods, *J. Chem. Soc., Perkin Trans. 2,* 1999, 493–503.

34 (a) C. Hazra, S. Sarkar, B. Meesaragandla and V. Mahalingam, *Dalton Trans.*, 2013, ***42***, 11981-11986; (b) T. Tachikawa, T. Ishigaki, J.-G. Li, M. Fujitsuka and T. Majima, *Angew. Chem. Int. Ed.,* 2008, ***47***, 5348-5352.

35 (a) D. Parker and J. A. G. Williams, *J. Chem. Soc. Dalton Trans.,* 1996, 3613-3628; (b) B. Sitharaman, S. Rajamani and P. K. Avti, *Chem. Commun.,* 2011, ***47***, 1607–1609; (c) S. Deslandes, C. Galaup, R. Poole, B. M. Voegtlé, S. Soldevila, N. Leygue, H. Bazin, L. Lamarque and C. Picard, *Org. Biomol. Chem.,* 2012, ***10***, 8509–8523.

View Article Online
DOI: 10.1039/C6DT01917J

36 (a) J.-C. G. Bünzli, *Chem. Rev.,* 2010, ***110***, 2729–2755, (b) J. Shen , L.-D. Sun and C.-H. Yan, *Dalton Trans.,* 2008, 5687-5697.
37 L.-M. Fu, X.-F. Wen, X.-C. Ai, Y. Sun, Y.-S. Wu, J.-P. Zhang, and Y. Wang, *Angew. Chem. Int. Ed.,* 2005, ***44***, 747 –750; (b) A. D'Aléo, A. Picot, P. L. Baldeck, C. Andraud, and O. Maury, *Inorg. Chem.,* 2008, ***47***, 10269–10279; (c) Z.-J. Hu, X.-H. Tian, X.-H. Zhao, P. Wang, Q. Zhang, P.-P. Sun, J.-Y. Wu, J.-X. Yang and Y.-P. Tian, *Chem. Commun.,* 2011, ***47***, 12467–12469.
38 (a) A. Picot, A. D'Aléo, P. L. Baldeck, A. Grichine, A. Duperray, C. Andraud and O. Maury, *J. Am. Chem. Soc.,* 2008, ***130***, 1532-1533; (b) W.-S. Lo, W.-M. Kwok, G.-L. Law, C.-T. Yeung, C. T.-L. Chan, H.-L. Yeung, H.-K. Kong, C.-H. Chen, M. B. Murphy, K.-L. Wong, and W.-T. Wong, *Inorg. Chem.,* 2011, ***50***, 5309–5311; (c) S. Sandoval, J. Yang, J. G. Alfaro, A. Liberman, M. Makale, C. E. Chiang, I. K. Schuller, A. C. Kummel and W. C. Trogler, *Chem. Mater.,* 2012, ***24***, 4222−4230.

View Article Online
DOI: 10.1039/C6DT01917J

TOC

Novel LaF_3:Eu(5%) nanocrystals containing partially-capped 1,10-phenanthroline ligands have been obtained, which display intense phen-sensitized europium emission in water and multiple lifetimes from Eu^{3+}-dopant sites.

View Article Online
DOI: 10.1039/C6DT01917J

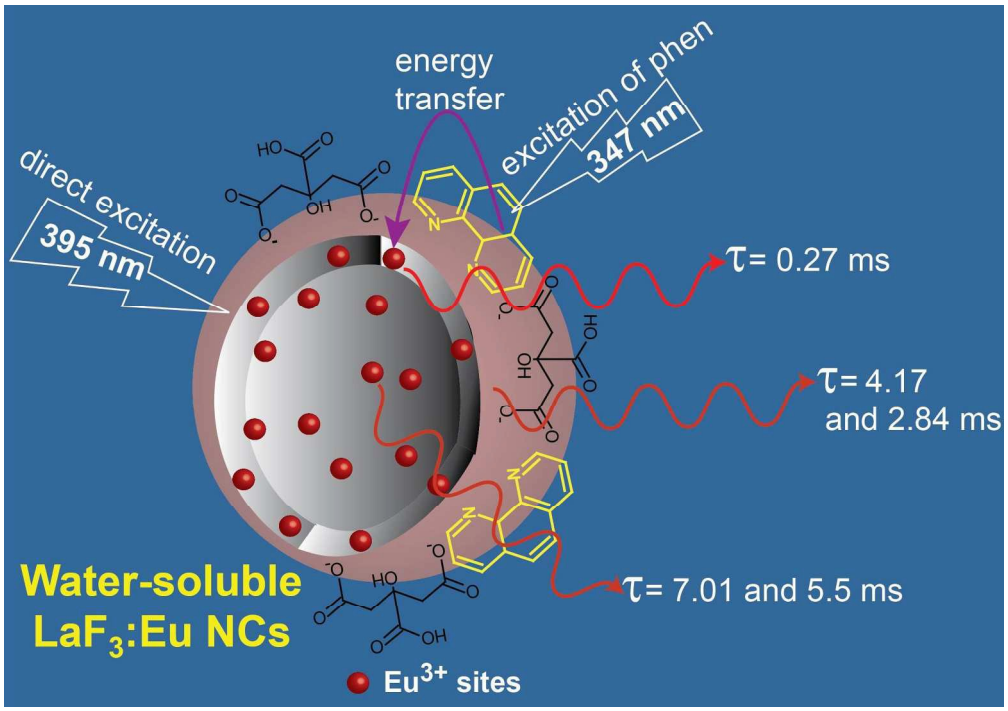

197x138mm (300 x 300 DPI)